ELSEVIER

Journal of Hazardous Materials B87 (2001) 73–98

Journal of Hazardous Materials

www.elsevier.com/locate/jhazmat

# Development of adsorptive removal process for treatment of explosives contaminated wastewater using activated carbon

Chitra Rajagopal, J.C. Kapoor*

*Centre for Environment and Explosive Safety, Ministry of Defence, Metcalfe House, DRDO, New Delhi 110054, India*

Received 30 September 2000; received in revised form 18 January 2001; accepted 1 February 2001

**Abstract**

The adsorption characteristics of nitro-organics such as trinitro-toluene (TNT), dinitro-toluene (DNT) and nitrobenzene (NB) on granular activated carbon (GAC) were studied to understand their dynamic adsorption behaviour for dilute aqueous solutions. A model was developed to predict the dynamics of the adsorption process and the effect of various design and operating parameters on adsorption characteristics. The model predictions would provide inputs to design of bench scale and pilot plant scale experiments.

Section 2 of the paper describes the assumptions, predictions, development of the model and its validation with experimental data generated during bench scale and pilot plant trials. Section 3 presents the breakthrough characteristics obtained by conducting experimental runs for GAC of different surface areas from 650 to 1500 $m^2/g$, hydraulic loading rates (HLR) ranging between 12 and 24 $m^3/h/m^2$, feed concentrations from 50 to 130 mg/l and bed heights between 300 and 1000 mm for TNT, DNT and NB solutions. The effect of these independent parameters on the breakthrough time, adsorption capacity and the minimum concentration achieved in the effluent was studied and the results obtained are presented in this paper. These indicate that the adsorption capacity goes though a maximum when studied as a function of HLR and feed concentration. The adsorption capacity per unit surface area also shows a maximum around 1000 $m^2/g$. The minimum bed height required for meeting environmental effluent discharge limit of 1 ppm was experimentally found to be about 800 mm. These results compare well with the predictions based on the model developed for column adsorption process. Data from these experimental runs and the model predictions have been used to optimise various parameters for the design of a pilot plant unit with 200 l per hour capacity. © 2001 Elsevier Science B.V. All rights reserved.

*Keywords:* Activated carbon; Nitro-organics; Dynamic adsorption; Model

* Corresponding author. Tel.: +91-11-391-1035; fax: +91-11-391-4960.

0304-3894/01/$ – see front matter © 2001 Elsevier Science B.V. All rights reserved.
PII: S0304-3894(01)00179-0

## 1. Introduction

The nitro-organics found in the waste streams from trinitro-toluene (TNT) manufacturing plants, are toxic in nature in addition to being suspected carcinogens. These waste streams, if released untreated, may result in contamination of the soil and ground water, thereby affecting the health of humans and may have a detrimental effect on the environment. Therefore, concentration of total nitro-organics in the effluent waste waters needs to be brought down so as to meet a low interim discharge limit of 1 ppm of total nitrobodies [1–3].

Conventional industrial effluent treatment schemes have not been found suitable for bringing down the concentration in the wastewater to the required low limits. Various other techniques such as oxidation with hydrogen peroxide/ozone, adsorption, photocatalytic oxidation and biological degradation have been studied. Of these techniques, adsorption on granular activated carbon (GAC) appears promising and pilot scale plants based on this technique are operational in some of the US military establishments [4]. Hence, work on adsorption characterisitcs of these nitro-organics on different grades on activated carbon was initiated to develop a continuous adsorptive removal process for application in defence. As a first step, static isotherm studies were carried out to select the most suitable grade.

Dynamic studies for adsorption of TNT, Dinitro-toluene (DNT), nitrobenzene (NB) and their mixture from aqueous solutions on GAC beds in columns have been carried out to generate data for design of pilot plants and eventual application to continuous treatment of effluents from explosive manufacturing plants. A model describing the dynamics of the adsorption process was developed to predict the effect of process and operational variables. This facilitated design of bench scale and pilot programmes.

Section 2 of this paper presents the model development, including assumptions and predictions. The model validation using experimental data from dynamic studies described in Section 3, is also presented. Section 3 shows the results of studies on the dynamic adsorption behaviour of GAC in column mode operation on a bench scale unit using two columns in series with a third as standby.

## 2. Model development and predictions

### *2.1. Dynamics of column adsorption*

#### *2.1.1. Static versus dynamic adsorption*

In static equilibrium adsorption, the same solution remains in contact with a given quantity of adsorbent. As the amount of solute adsorbed on the GAC increases and the solute concentration in solution reduces, the driving force for adsorption decreases with time accompanied by a reduction in the adsorption capacity. The adsorption process continues however, till an equilibrium between the solute concentration in solution, and the solute adsorbed per unit weight of adsorbent, is reached. This equilibrium established is static in character, as it does not change further with time. The static equilibrium behaviour is characteristic of the nature of the adsorbent, the adsorbate, the solvent and the temperature. In dynamic column adsorption, solution continuously enters and leaves the column, so that the GAC in the column meets fresh solution each time. Depending on the fluid velocity

and bed height, the contact time for adsorption will vary. However, complete equilibrium is never established at any stage between the solute in solution and the amount adsorbed. There is at the most, an approach to equilibrium, which is termed as dynamic equilibrium, as it has to be continuously re-established each time the adsorbent meets fresh solution.

#### *2.1.2. Establishment of an adsorption zone*

The fluid entering the column passes initially though a virgin adsorbent bed. The foremost part of the adsorbent bed, which meets the entering solution, adsorbs the solute rapidly and effectively, during the start of the run. Whatever little solute remains in the solution is removed in the lower part of the bed, so that the fluid emerging from the bed is entirely free of solute. With time, as the cumulative volume of fluid which has passed though the bed increases, an adsorption zone is established, where the bulk of the adsorption takes place and across which the concentration varies from about 100% feed concentration (corresponding to complete saturation) to nearly 0% feed concentration (corresponding to virgin adsorbent). This adsorption zone moves down the column with time as the feed to the column continues. Eventually, the end of the adsorption zone touches bed bottom and some of the solute in the fluid emerges unadsorbed from the column. The solute concentration in the treated effluent reaches an appreciable value for the first time in the run. As the run continues, the adsorption zone starts moving out of the column and the effluent concentration starts rising with time. This is termed as breakpoint. For practical purposes, a specific concentration, of interest, is taken as the breakthrough concentration and the time taken for effluent concentration to reach this value is called the breakthrough time and the effluent concentration history after breakpoint is termed the breakthrough curve. The breakthrough curve for most solute-adsorbent systems, after an effluent concentration of 50% is reached, is a mirror image of the curve obtained before this point. Therefore, for ease of calculation of adsorption capacity of the adsorbent, standard practice [6] is to fix the breakthrough concentration at 50% of feed concentration. When the adsorption zone moves out of the bed, the bed is completely saturated, the net adsorption in the bed is zero and the effluent concentration equals the feed concentration.

Behaviour of any solute in an adsorption column is thus characterised by the dynamics of the adsorption front in the column and the total adsorption is quantitatively characterised by the breakthrough of the solute at the end of the adsorption cycle.

### *2.2. Model development and adsorption column design*

The dynamic adsorption process has been modelled by breaking down the mechanism described above into discrete steps. The algorithm followed for the model development is given in Fig. 1. This model generates output in the form of following parameters which can be used in design of adsorption column.

1. Length of the adsorption zone.
2. Optimal residence time within the column.
3. Optimal surface area of adsorbent.
4. Optimal ratio of adsorbent particle/column diameter.
5. Pressure drop across bed.

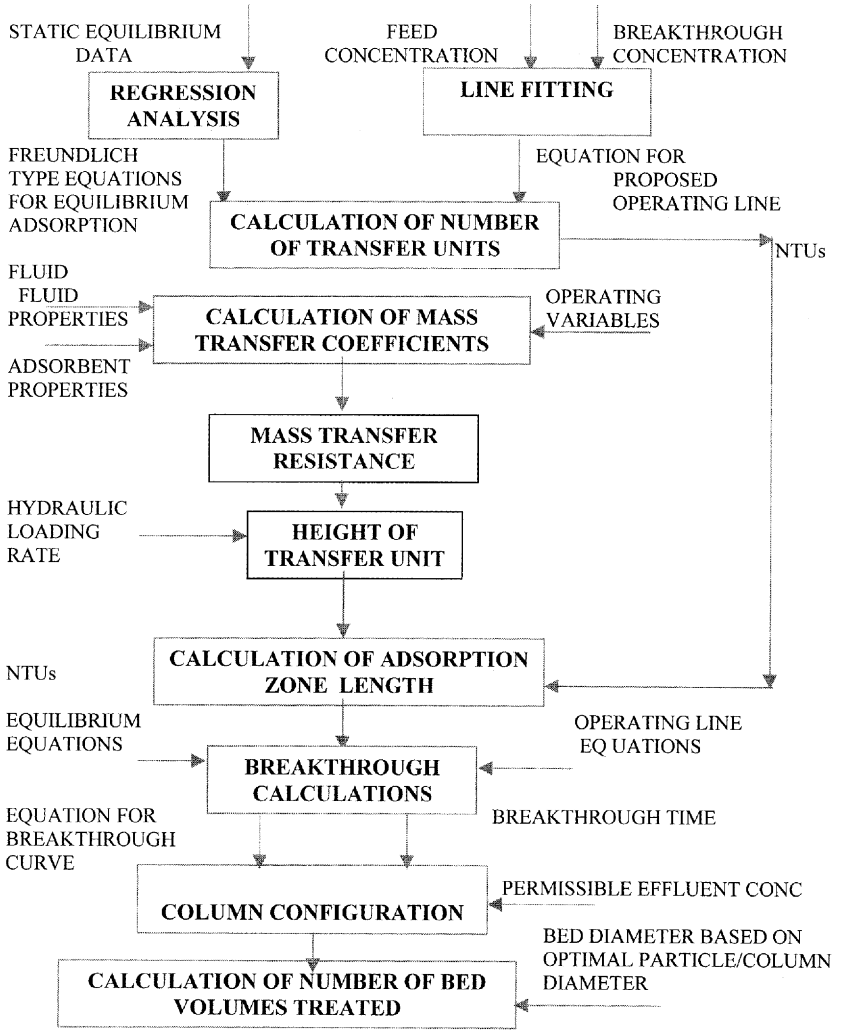


Fig. 1. Algorithm for model development.

### 2.2.1. *Design fundamentals*

The basis behind adsorption column design is two-fold [6,7].

1. Minimise solute concentration in treated effluent, to below environmentally permissible limits.
2. Minimise adsorbent usage by maximising its utilisation.

The data required for column design are summarised below.

1. Equilibrium isotherm data for the solute-adsorbent system of interest.
2. Feed and effluent concentrations.

3. Kinetic rate data.
4. Adsorbent characterisitcs — particle size, bulk density and porosity.
5. Properties of solution — density, viscosity, solute diffusivity.
6. Required effluent treatment rate, i.e. feed flow rate to column.

The design output should predict the following factors.

1. Adsorption zone length.
2. Breakthrough data.
3. Optimal hydraulic loading rate (HLR) (flow rate per unit cross-sectional area of bed) and therefore the column diameter.
4. Minimum length of bed.
5. Fractional unsaturation of bed at breakthrough.
6. Time for breakthrough and for complete exhaustion of adsorbent bed.
7. Adsorption capacity of bed.
8. Number of bed volumes that can be treated.

*2.2.2. Design methodology*

Design of the adsorption column will involve the following steps.

*2.2.2.1. Calculation of number of transfer units (NTUs).* The NTUs required for achieving the desired effluent concentrations under the given conditions of flow and feed concentration, will depend on the available driving force for mass transfer. The magnitude of the driving force will depend on the difference between the actual and equilibrium concentrations of the solute, $c$ and $c^*$, respectively. The NTU maybe calculated as follows.

$$\mathrm{NTU} = \int_{c_{\mathrm{out}}}^{c_{\mathrm{in}}} \frac{\mathrm{d}c}{c - c^*} \tag{1}$$

where $c_{\mathrm{in}}$ and $c_{\mathrm{out}}$ are the feed and effluent concentrations, respectively.

Equation of operating line, for the specified feed and desired effluent concentrations, the corresponding equilibrium $q$ values, $q_{\mathrm{in}}$ and $q_{\mathrm{out}}$, may be obtained from the equilibrium curve [1,2]. The equation for the operating line is then given by

$$q = \frac{q_{\mathrm{in}} - q_{\mathrm{out}}}{c_{\mathrm{in}} - c_{\mathrm{out}}}(c - c_{\mathrm{out}}) + q_{\mathrm{out}} \tag{2}$$

Value of $q$ corresponding to any $c$ on the operating line can be read calculated from the above equation. Further, the equilibrium concentration, $c^*$, corresponding to each $q$ can be read either from the equilibrium curve or may be calculated from Eq. (3) obtained by regression analysis of experimentally collected equilibrium data, where $K$ is the equilibrium constant and $1/n$ is the concentration exponent.

$$c^* = \left(\frac{q}{K}\right)^{1/n} \tag{3}$$

*2.2.2.1.1. Fitting of static equilibrium equations by regression analysis of equilibrium isotherm adsorption data.* Isotherm data for the nitro-organics of interest was obtained

Table 1
Results of regression analysis of equilibrium isotherm data

| Nitro-organic | GAC grade ($m^2/g$) | Feed concentration (mg/l) | $K$ | $1/n$ | Range (mg/l) |
|---|---|---|---|---|---|
| Trinitro-toluene | 650 | 122.5 | 20.5 | 0.294 | 0–0.5 |
| | | 92 | 75.86 | 0.2 | 0–92 |
| | 1000 | 100 | 0.00139 | 9.8 | 0–3 |
| | | | 57.4 | 0.32 | 3–100 |
| | | 110.8 | 32.8 | 0.42 | 0–110.8 |
| | 1350 | 94.5 | 14.54 | 0.75 | 0–94.5 |
| Dinitro-toluene | | | 0.00038 | 5 | <8.32 |
| | 1000 | 60 | $c_e = 8.32$ | | 8.32 |
| | | | 5.0 | 1.063 | >8.32 |
| Nitrobenzene | 650 | 142.2 | 23.5 | 0.458 | 0–142.2 |
| | 1000 | 100 | 3.4 | 1.8 | ≤6 |
| | | | 18.2 | 1.0 | >6 |
| | 1350 | 133 | 1.78 | 2.0 | ≤8 |
| | | | 23.4 | 0.8 | >8 |

from static isotherm studies [5]. This data relates the amount adsorbed per unit mass of adsorbate, $q_e$, to the equilibrium concentration of the nitro-organic in solution, $c^*$, for NB, TNT and DNT.

Regression analysis of this data was carried out to fit a Freundlich-type equation of the form

$$q_e = Kc^{*(1/n)} \tag{4}$$

A logarithmic form of the equation was found convenient for curve-fitting.

$$\log q_e = \frac{1}{n} \log c^* + \log K \tag{5}$$

The slope of the $\log q_e$ versus $\log c^*$ curve gives the value of $1/n$, while the $y$-intercept gives the value of $\log K$. The plots show two clear trends — one for lower concentration range (below 5 mg/l) and one for higher concentrations. Therefore, two separate equations were fitted for the two ranges. Table 1 gives the constants for each case. Values of $c$ are selected at regular intervals over the whole range from $c_{in}$ to $c_{out}$. With the help of Eqs. (4) and (5), $c^*$ corresponding to each $c$ is noted. From the values of $c$ and $c^*$, $1/(c - c^*)$ is calculated. Individual values of $1/(c - c^*)$ are then plotted against the corresponding $c$ values to obtain a curve. The area under the curve from $c_{in}$ to $c_{out}$ gives the NTUs. Table 2 gives the calculated NTUs for TNT, NB and DNT.

*2.2.2.2. Calculation of height of a transfer unit (HTU).* The HTU depends on the overall resistance to adsorptive mass transfer offered by the system. The kinetic behaviour will determine this resistance. The overall resistance can be broken up into various components. These can be identified by looking at the mass transfer route. The solute from the solution is adsorbed onto the adsorbent though the following steps.

Table 2
Input data for design calculations

| | |
|---|---|
| GAC characteristics[a] | |
| BET surface area ($m^2/g$) | 650–1500 |
| Particle size (mesh) | 8–20 |
| Average particle size (mm) | 1.18 |
| Particle density ($g/cm^3$) | 0.85 |
| Bulk density ($g/cm^3$) | 0.5 (0.4–0.57 g/cc) |
| Particle diffusivity ($cm^2/s$) | $10^{-7}$ |
| Min iodine No. (mg/g) | 950 |
| Min $CCl_4$ adsorption (%) | 50 |
| Min hardness No. (%) | 95 |
| Max ash content (%) | 3 |
| Max moisture content (%) | 5 |
| pH | Alkaline |
| Fluid characteristics | |
| Fluid/solvent | Water |
| Density ($g/cm^3$) | 1.0 |
| Viscosity (P) | 0.01 |
| Diffusivity ($cm^2/s$) | $10^{-5}$ |
| Packed bed characteristics | |
| Porosity, $\varepsilon$ | 0.412 |
| Specific surface area, $a_p$ (bed volume) ($cm^2/cm^3$) | 7 |
| Independent variables | |
| GAC grades (surface area) ($m^2/g$) | 650/1000/1500 |
| Hydraulic loading rate ($m^3/h/m^2$) | 12/16/24 |
| Feed concentration (mg/l) | 54/100/120 |
| GAC bed height (mm) | 300/600 |

[a] From M/s. Active Carbon, Hyderabad.

1. Fluid phase diffusion of solute though the boundary layer surrounding each adsorbent particle.
2. Diffusion of solute though the pores of the adsorbent.
3. Particle phase diffusion or inter-particle transmigration of solute.
4. Adsorption on walls or surface of pores.
5. Axial dispersion or mixing effects.

Of the above, steps 2 and 3, act in parallel, while step 1 is in series with the former. Step 4 is basically a reaction step and can be neglected for purposes of calculating mass transfer resistance. Step 5 comes into play only in cases of turbulent and non-uniform flow conditions in the adsorption column. Steps 1 and 5 are fluid side effects, 2 and 3 are termed particle side effects and are independent of the hydro-dynamic conditions existing in the column.

- Step 1: fluid phase diffusion

The fluid phase mass transfer coefficient, $k_f$, can be calculated from the following equation [1] for adsorption from dilute aqueous solutions with porosity equal to 0.4.

$$k_f a_p = \frac{2.62(D_f Q/A)^{1/2}}{d_p^{1.5}} \tag{6}$$

where $k_f$ is the mass transfer coefficient (cm/s); $a_p$ the external area of adsorbent particle per unit volume of bed ($cm^2/cm^3$); $D_f$ the fluid diffusivity ($cm^2/s$) (can be considered concentration independent for fixed bed operations); $Q$ the fluid flow rate ($cm^3/s$); $A$ the cross-sectional area of the bed ($cm^2$); $d_p$ the adsorbent particle diameter (cm); $a_p$ may be calculated from

$$a_p = \frac{6(1-\varepsilon)}{d_p} \tag{7}$$

$\varepsilon$ is the porosity given by

$$\varepsilon = \frac{\rho_p - \rho_b}{\rho_p} \tag{8}$$

where $\rho_b$ and $\rho_p$ are the bulk and particle densities, respectively.

- Step 2: particle side diffusion

The pore and particle side mass transfer coefficients are related to the fluid and particle diffusivities, respectively. The pore side mass transfer coefficient is given by

$$k_{po} a_p = \frac{60 D_{po}}{d_p^2}(1-\varepsilon) \tag{9a}$$

where $k_{po}$ and $D_{po}$ are the pore mass transfer coefficients and diffusivity, respectively, and $d_p$ the effective spherical particle diameter.

$D_{po}$ for liquids is given by

$$D_{po} = \frac{D_f \chi}{\sqrt{\tau}} \tag{9b}$$

where $\chi$ and $\tau$ are the internal porosity and tortuosity, taken as 0.6 and 4, respectively.

The particle side mass transfer coefficient is given by

$$k_p a_p = \frac{60 D_p}{d_p^2} \tag{10}$$

where $D_p$ is the particle side diffusivity.

Net pore and particle resistance

$$k_{op} a_p = k_p a_p + k_{po} a_p \tag{11}$$

where $k_{op}$ is the overall particle phase mass transfer coefficient.

- Step 3

The resistance due to axial dispersion is given by $1/k_d a_d$, where $k_d$ and $a_d$ are the mass transfer coefficient and the mass transfer area corresponding to axial dispersion and is

given by

$$\frac{1}{k_d a_d} = \frac{A}{LQ} \tag{12}$$

where $Q$ is the volumetric flow rate, $A$ the cross-sectional area of flow and $L$ the mixing length, given by

$$L = \frac{d_p}{Pe} + \frac{D_f}{2(Q/A)} \tag{13}$$

where $Pe$ is the Peclet number, which varies with the particle Reynolds number, $Re_p$, given by

$$Re_p = \frac{d_p \rho_f Q}{A\mu} \tag{14}$$

where $\rho_f$ is the fluid density.

For $Re_p < 20$, $Pe = 0.5$

Combined mass transfer resistance

$$\frac{1}{k_o a_p} = \frac{b_f}{k_f a_p} + \frac{1}{k_{op} a_p} + \frac{1}{k_d a_p} \tag{15}$$

where $b_f$ is a factor which takes care of the non-linearity in the addition of the individual resistances. This may be given by the average slope of the equilibrium curve in the concentration range of interest or as a function of fluid Reynolds number.

HTU is given by

$$\text{HTU} = \frac{G}{k_o a_p} \tag{16}$$

where $G$ is the HLR (volumetric flow rate/cross-sectional area of flow) (cm/s).

*2.2.2.3. Length of the adsorption zone ($z_a$).* The length of the adsorption zone, $z_a$, is given by the product of the NTUs and the height of the transfer unit

$$z_a = \text{NTU} \times \text{HTU} \tag{17}$$

*2.2.2.4. Breakthrough calculations.* The time to breakthrough is an important parameter for planning the adsorption cycle. The time to breakpoint, $t_b$, of the bed can be found by a mass balance of adsorbate/solute across the adsorption zone.

$$\text{solute}_{in} - \text{solute}_{out} = \text{solute absorbed on bed}$$

$$F\varepsilon(c_{in} - c_{out})t_b = (z - fz_a)q_e A(1-\varepsilon)\rho_b \tag{18}$$

where $z$ is the length of the bed; $f$ the fractional unsaturation of the bed at breakpoint and can be estimated graphically from area above the curve in $c/c_{in}$ versus $z/z_a$.

Fig. 2a–c give the $c/c_{in}$ versus $z/z_a$ curves for TNT, NB and DNT.

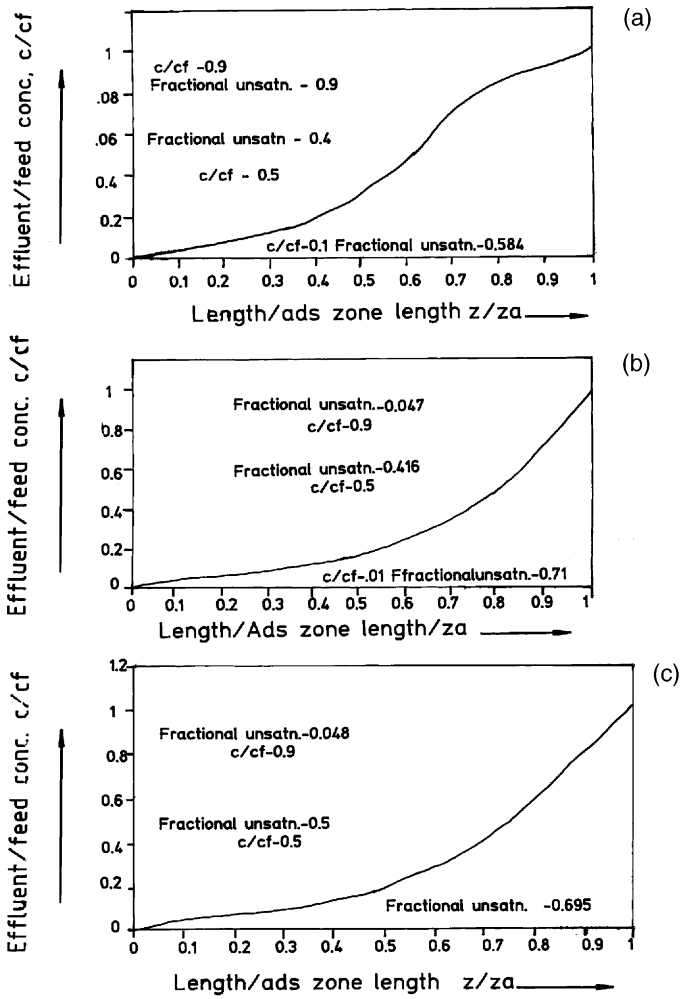


Fig. 2. Fractional unsaturation in column at breakthrough predicted by model: breakthrough curves for (a) NB; (b) TNT; (c) DNT.

From Eq. (19), $t_b$ is given by

$$t_b = \frac{(z - fz_a)q_e A(1-\varepsilon)\rho_b}{F\varepsilon c_{in}} \tag{19}$$

Here, $z/z_a$ corresponding to each value of $c/c_{in}$ for $z < z_a$, is given by

$$\frac{z}{z_a} = \frac{\int_{c_{out}}^{c} dc/(c-c^*)}{\int_{c_{out}}^{cE} dc/(c-c^*)} \tag{20}$$

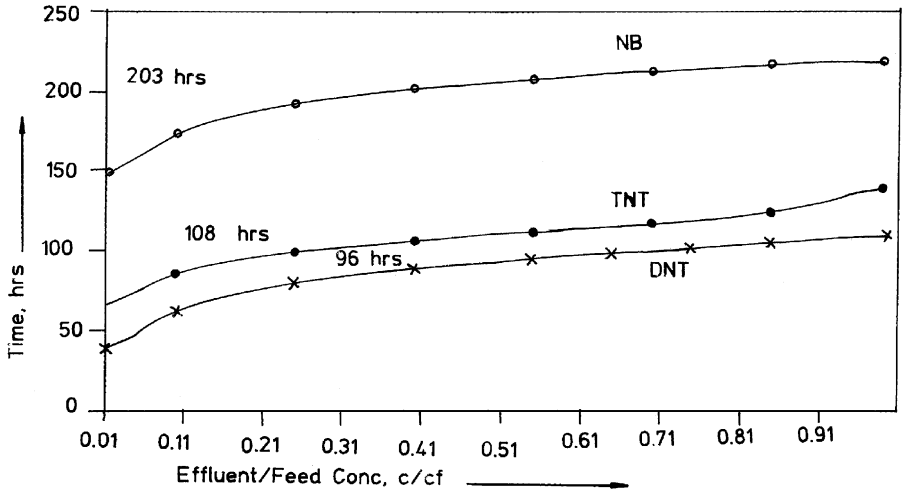


Fig. 3. Effluent concentration history.

where $c_E$ is the concentration at 90% of feed concentration (for practical purposes, $c_E$ is taken instead of complete saturation, corresponding to 100% feed concentration. As the effluent concentration approaches the feed concentration exponentially, since this would take a very long time). And $t$ is related to $z$ by

$$\frac{t - t_b}{t_a} = \frac{z}{z_a} \tag{21}$$

where $t_a$ is the time taken by the adsorption zone to move out of the column after breakthrough and is calculated by imagining that the sorption zone is being brought to rest by an equal and opposite velocity, $u_w$.

$$u_w \rho_b A = F c_{in} \tag{22}$$

$$t_a = \frac{z_a}{u_w} \tag{23}$$

$$t = \frac{z}{z_a} t_b, \quad \text{for} \quad t < t_b \tag{24}$$

$$t = t_b + \frac{z}{z_a} t_a \tag{25}$$

From Eqs. (21)–(26), $t$ corresponding to each value of c or $c/c_{in}$ can be calculated. A plot of $c/c_{in}$ versus $t$ will give the breakthrough curve. Figs. 2 and 3 gives the breakthrough curves for TNT, NB and DNT based on the model predictions.

*2.2.2.5. Pressure drop calculations.* The pressure drop across the bed is given by

$$\Delta p = \frac{K' \mu Q L_c}{d_p^2 d_c} \tag{26}$$

Table 3
Model predictions

| Nitro-organic | NTU (units) | Fractional unsaturation | Fluid diffusivity ($cm^2/s$) | | Hydraulic loading rate ($m^3/h/m^2$) | | |
|---|---|---|---|---|---|---|---|
| | | | | | 15 | 21 | 27 |
| Nitrobenzene | | | | $b_f$ | 1.0 | 1.0 | 1.0 |
| | | | | HTU (mm) | 37 | 51 | 60 |
| | 1.2 | 0.58 | 1.5E-06 | $z_a$ (mm) | 44 | 59 | 72 |
| Feed concentration (200 mg/l) | | | 300 mm | $t_b$ (h) | 19.5 | 13.1 | 9.2 |
| Trinitrotoluene | | | | $b_f$ | 3.4 | 1.0 | 1.0 |
| | | | | HTU (mm) | 296 | 130 | 175 |
| | 1.74 | 0.4 | 1.5E-06 | $z_a$ (mm) | 504 | 226 | 305 |
| Feed concentration (100 mg/l) | | | 300 mm | $t_b$ (h) | 15 | 24.7 | 14.2 |
| | | | 600 mm | $t_b$ (h) | 47 | 58.3 | 35 |
| Dinitrotoluene | | | | $b_f$ | 1.86 | 1.0 | 1.0 |
| | | | | HTU (mm) | 204 | 154 | 160 |
| | 1.74 | 0.61 | 1.1E-06 | $z_a$ (mm) | 383 | 300 | 310 |
| Feed concentration (33 mg/l) | | | 300 mm | $t_b$ (h) | 21 | 27.8 | 22 |
| GAC grade | IV (1000 $m^2/g$) | | | | | | |
| Feed concentration | 100 mg/l | | | | | | |
| Bed height | 300 mm | | | | | | |

Table 4
Output-design parameters

| | |
|---|---|
| Bed length (min) (mm) | 800 |
| Number of columns (in series) | 2 |
| Hydraulic loading rate ($m^3/h/m^2$) | 16 |

where $K'$ is a constant; $\Delta p$ the pressure drop; $\mu$ the viscosity; $Q$ the flow rate; $L_c$ the bed depth; $d_p$ the mean particle diameter; $d_c$ the column diameter.

### 2.2.3. *Example design calculations*

The following example serves to demonstrate the use of the above procedure for design of the column for adsorption of various nitro-organics mentioned in Table 1. The data used for the design calculations is given in Table 2. Table 3 gives the model predictions for this data. The output generated in terms of the design parameters for the plant, based on these calculations, is given in Table 4.

## 3. Bench scale studies

Preliminary experiments were conducted using a dynamic, multiple column adsorption system to study the feasibility of achieving effluent concentrations which meet the regulatory

discharge limits. Dynamic column experiments using 25 mm diameter column were used to arrive at the range of experimental conditions and to standardise equipment and required accessories, frequencies and procedures for sampling and analytical procedures. This was followed by bench scale experiments with 50 mm diameter adsorption columns for which the data is presented in this paper. The experimental results are compared with model predictions.

The main objectives of these studies are to optimise critical process and operating variables so as to minimise the concentration of pollutant in treated effluent and to maximise the adsorption capacity of the GAC, thereby reducing the carbon usage and decreasing operational cost. This has been achieved by studying effect of individual parameters, which are given below, on the adsorption characteristics.

1. Effect of GAC surface area.
2. Effect of feed concentration.
3. Effect of HLR.
4. GAC bed height.

The results of these experimental studies were combined to get the optimum operating conditions for the pilot plant.

### 3.1. Experimental details

The experimental arrangement is shown in Fig. 4 and consists of two columns of borosilicate glass of 50 mm diameter arranged in series. Feed solution of 100 mg/l concentration stored in an overhead tank of 200 l capacity with overflow arrangement, was gravity fed

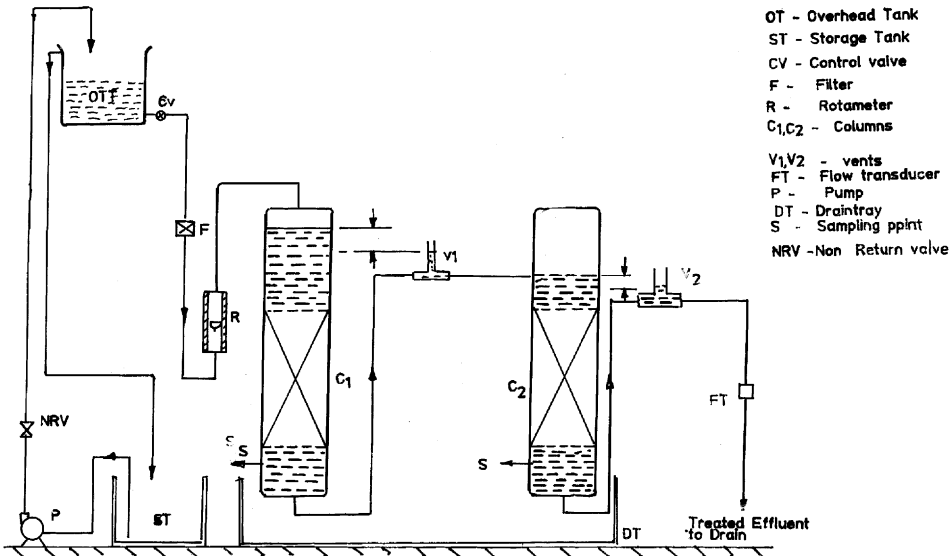


Fig. 4. Experimental set-up for column studies.

to the columns. Atmospheric vents, at suitable heights, were provided at the outlet tubings from both columns. The differential head between the vent tube and the liquid level in the columns was used as a measure of the pressure drop across the bed. Sampling points before and after the columns were also provided for drawing the effluent samples at regular intervals. Effluent after passing though the columns was discharged into a sump below the columns.

GAC was packed in the columns under wet conditions. Previously wetted degassed activated carbon was packed to desired height in water filled columns and was kept submerged throughout the runs to avoid air entrapment in the bed. Two of these columns were operated in series, while a third served as a standby to replace the first column when it gets saturated. The GAC bed was supported on perforated plates. The column was mounted vertically and the feed was gravity fed into the first column from an overhead tank. The effluent from the first column formed the influent to the second column. The operation was in the downflow plug mode.

The solution in (T2) was maintained at a constant level by an overflow arrangement in order to ensure constant feed rate to the column. A filter (F1) in the feed line to remove suspended particulates, which may clog the GAC, a control valve (CV) to regulate the flow and a rotameter (*R*) to monitor the flow rate, were incorporated in the feed line to the first column.

The characteristics of the GAC used in these studies were given in Table 1 in Section 2. The key independent and dependant experimental variables and the range of variation of operating variables studied are given in Table 5.

Data collected from these experiments have been used to calculate the following variables using empirical equations as shown. Adsorption capacity of GAC, calculated as below

$$\text{adsorption capacity} = \frac{\text{nitrobody adsorbed on GAC bed}}{\text{mass of GAC in bed}} = \frac{\text{breakthrough time} \times \text{flow rate} \times \text{feed concentration}}{\text{mass of GAC in bed}}$$

Table 5
Range of experimental conditions

| | |
|---|---|
| GAC surface area (sqm/gm) | 650–1500 |
| GAC bed height (mm) | 200–1100 |
| Hydraulic loading rate ($m^3/h/m^2$) | 11–40 |
| Nitro-organics studied | TNT, DNT, NB, mixtures of TNT, DNT, NB |
| Feed concentrations | |
| Single component solutions (mg/l) | 30–130l |
| Mixtures (total concentration) (mg/l) | 100 |
| Measured Variables | |
| Pressure drop across bed | |
| Nitrobody concentration in treated effluent at regular time intervals | |
| Minimum achievable concentration in treated effluent | |

### 3.1.1. Analytical methods

*3.1.1.1. Single component solutions.* Single component solutions of NB, DNT and TNT were analysed using a double beam GBC 916 UV–VIS spectrophotometer at their respective wavelengths corresponding to maximum absorption.

*3.1.1.2. Mixtures.* Solutions of mixtures were analysed using HPLC and by UV–VIS using a methodology developed for this purpose.

- HPLC analysis

The analysis involved the following steps.

1. Preparation of standard solution
   A known weight of standard reference materials (SRM) from HE Factory, Kirkee, Pune, dried to constant weight was dissolved in minimum quantity of acetone (Merck AR quality). This solution was added to hot water and made up to 100 ml in a volumetric flask. Aliquots of SRM acetone solutions were diluted with Milli-Q purified water to prepare standards of known concentrations for calibration.
2. Sample treatment
   All the aqueous samples for direct injection analysis were filtered though millipore filters (0.45 μm) to remove any suspended particulates.
3. Analysis
   Mixtures of NB, DNT and TNT were analysed at all levels by direct injection using a reversed phase HPLC system (model Perkin-Elmer 1022 L) and a photodiode array detector (model Perkin-Elmer 235 C).

Analytical conditions for HPLC analysis were as follows.

| | |
|---|---|
| Mobile phase | 35:65 acetonitrile and water |
| Flow rate | 1.6 ml/min |
| Column | Brownly spheri-10RP-18, 100 mm × 4.6 mm |
| Injection volume | 20 μl |
| Detector wavelength | 250 nm |
| Sensitivity | 0.2 (AUFS) |

- UV–VIS analysis

A new technique was developed to determine composition of two-component mixtures based on shift in $\lambda_{max}$ (wavelength corresponding to maximum absorption) with different compositions of the components [7]. This facilitated faster and more economical analysis of pilot plant effluents.

### 3.1.2. Experimental work-plan

A number of experiments were carried out in order to study the effect of each of the four operating variables.

- Set I

Effect of GAC surface area on adsorption capacity and minimum achievable effluent concentration, $c_e$ was studied on following grades of GAC.

1. Grade I: 1500 $m^2$/g.
2. Grade IV: 1000 $m^2$/g.
3. Grade VI: 650 $m^2$/g.

A GAC bed height of 300 mm was selected on the basis of the adsorption zone lengths predicted by model and adsorption study was carried out at a HLR of 11 $m^3/h/m^2$ and feed concentrations ranging from 54 to 120 mg/l. Based on these experiments, GAC with a surface area of 1000 $m^2$/g was optimised and used for further studies.

- Set II: effect of HLR

These experiments were conducted using GAC with surface area of 1000 $m^2$/g and two bed heights of 300 and 600 mm, at constant feed concentration of 100 mg/l and HLR ranging from 11 to 24 $m^3/h/m^2$. On the basis of these experiments, a HLR of 16 $m^3/h/m^2$ was selected for further studies.

- Set III: effect of bed height ($L_c$)

Breakthrough experiments were conducted at bed heights of 200, 300, 500, 700 and 1000 mm at constant feed concentration of 100 mg/l and at HLR of 16 $m^3/h/m^2$ optimised earlier to study the effect of $L_c$ on breakthrough period. A minimum bed height of 300 mm was selected on the basis of these experiments for further studies.

- Set IV: effect of feed concentration

The experiments were conducted at feed concentrations of 54, 100 and 132 mg/l for HLR of 16 $m^3/h/m^2$ and bed height of 300 mm.

## 4. Results and discussion

Though a large volume of data was collected on the dynamic adsorptive behaviour of a number of nitro-organics, the results of single component TNT solutions are presented in detail. The reason for this is that, being the main constituent of the actual effluent, TNT strongly influences and generally represents the overall adsorption behaviour of the effluent mixture. This is confirmed when the breakthrough behaviour of the mixture is compared with that of TNT (see Section 4.6). However, specific results for NB and DNT are presented wherever such results differ significantly from that of TNT and may have direct fallout on the design of the pilot plant. Effect of selected parameters on the breakthrough period, adsorption capacity and minimum effluent concentration are presented and discussed in the following sub-sections.

### 4.1. Effect of surface area

The ratio of effluent concentration at the outlet of the first column to the influent concentration, was plotted against the time period in order to obtain the breakthrough curves. The breakthrough curves become progressively flatter for higher GAC grades leading to larger breakthrough times. This behaviour can be explained on the basis of the larger surface area available for adsorption for higher grades of GAC, so that the time taken to saturate the bed is higher. This behaviour is corroborated by the results of static isotherm experiments. The observed plateau corresponds to the fractional saturation for monolayer adsorption. The adsorption capacity is found to increase with GAC surface area. The amount of TNT adsorbed per unit GAC surface area increases from about 0.11 mg/m$^3$ for grade VI (650 m$^2$/g) to 0.15 mg/m$^3$ for grade IV (1000 m$^2$/g) and 0.168 m$^2$/m$^3$ for grade I (1500 m$^2$/g), for a feed concentration of 100 mg/l. The curve shows a gradually decreasing slope with increasing GAC surface area up to 1000 m$^2$/g. This is explained on the basis of the micro and macropores structure of GAC. Though the surface area increases with the grade of carbon, the fraction of macropores, which contribute to the adsorption of a comparatively large molecule like TNT, and therefore the effective surface area, may not increase in the same proportion. The cost benefit ratio (cost of grade I GAC is nearly thrice that of grade IV for a 12% increase in adsorption capacity per unit surface area, whereas that for grade IV is less than twice that of grade VI for a 36% increase in adsorption capacity per unit surface area), justifies the selection of grade IV (1000 m$^2$/g) for further bench scale and pilot plant studies.

Fig. 5 shows the variation in minimum achievable concentration, $c_e$, with GAC surface area. It was found to decrease with surface area, with reduced slope of the curve, for GAC of 1000 m$^2$/g and above. The minimum $c_e$ reduces to below 1 mg/l for GAC surface area of 1350 m$^2$/g. However, bed height in these experiments was kept at 300 mm, equal to the adsorption zone length, in order to get shorter breakthrough times.

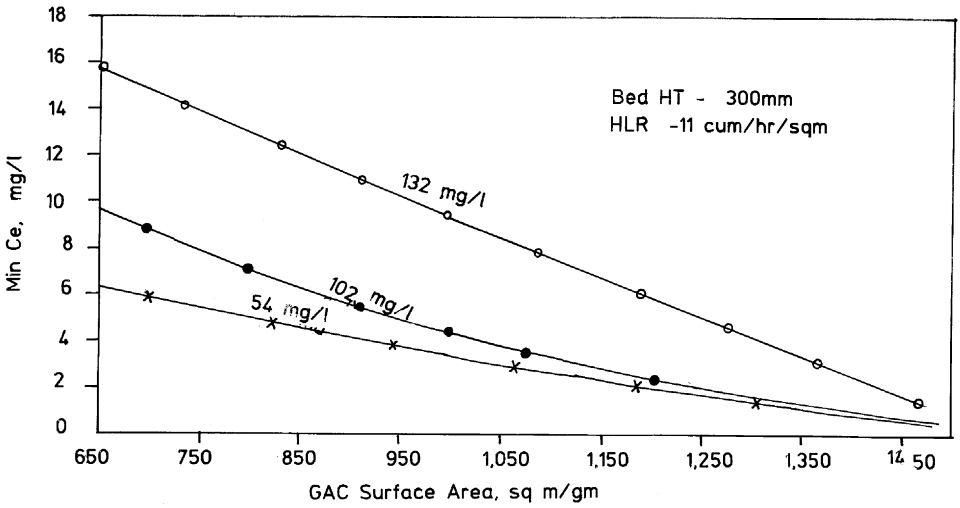


Fig. 5. Effect of GAC surface area on minimum effluent concentration for TNT.

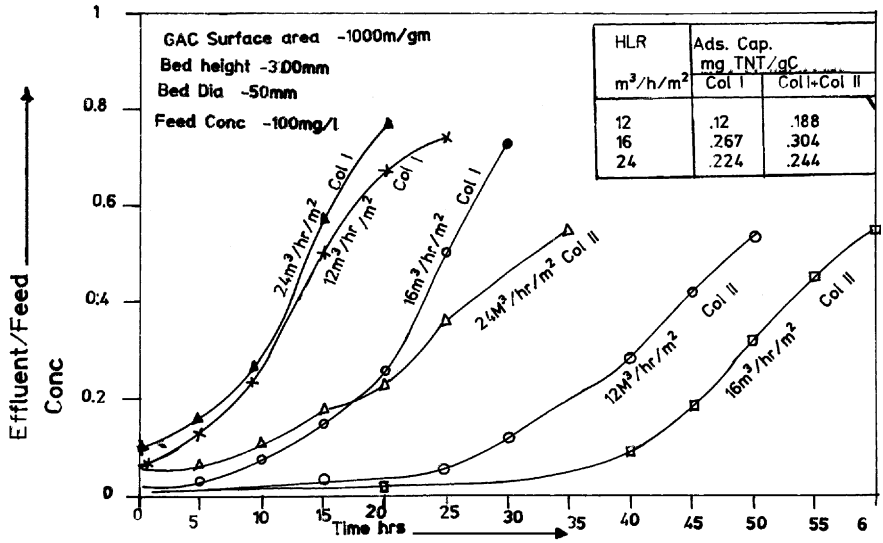


Fig. 6. TNT breakthrough curves at varying HLR.

### 4.2. Effect of hydraulic loading rate

Results of set II experiments on effect of HLR are plotted in Fig. 6, which depicts breakthrough curves for different flow rates/HLR. It is observed from the figure that, the slope of the breakthrough curve decreases as the HLR increases from 12 to 16 $m^3/h/m^2$. But, with further increase in HLR, the slope of the curve increases. The breakthrough time correspondingly increases up to 16 $m^3/h/m^2$, reaching about 25 h for an influent concentration of 100 mg/l, but decreases again to about 14 h at 24 $m^3/h/m^2$ a bed height of 300 mm. A similar variation is observed for a bed height of 600 mm with overall breakthrough time increasing from 47 h for 12 $m^3/h/m^2$ to 57 h for 16 $m^3/h/m^2$ and decreasing again to 30.5 h for 24 $m^3/h/m^2$. The adsorption capacity accordingly shows a maximum between 16 and 20 $m^3/h/m^2$. The curve for 300 mm bed height shows a flatter profile beyond 16 $m^3/h/m^2$ showing decreased sensitivity to HLR as compared to curve for 600 mm bed height which shows a distinct maximum in adsorption capacity.

The variation in the slope of the breakthrough curve and in the breakthrough time with HLR may be explained on the basis of adsorption mass transfer fundamentals (see Section 2.2.1). The speed at which the adsorption zone moves down the length of the bed increases with the HLR. But, the height of the zone depends not only on the HLR, but also on the overall resistance to mass transfer offered by the system. The overall resistance could be considered to arise from the fluid phase, the particle or sorbed phase and the pore side [6]. As the fluid phase resistance decreases with an increase in the HLR, while the particle and pore side resistances remain constant, the overall resistance also decreases. The net result of increased HLR and decreased resistance is a net decrease in the length of the adsorption zone. The effect of decreased adsorption zone length is a decrease in the rate of saturation

Table 6
Relative contribution from fluid and particle phase resistances to mass transfer

| Hydraulic loading rate, $G$ ($m^3/h/m^2$) | Overall mass transfer resistance, $R_o$ (s) | Contribution to overall resistance (%) | |
|---|---|---|---|
| | | Fluid | Particle |
| 12 | 35 | 37.5 | 62.5 |
| 16 | 6 | 32.0 | 68.0 |
| 24 | 9 | 28.0 | 72.0 |

of the bed and therefore, an increase in the breakthrough time, in spite of the increase in zone velocity. However, beyond a certain HLR, in the present case, 16 $m^3/h/m^2$, the effect of increase in zone speed is predominant, resulting in an increase in the rate of saturation of the bed (therefore, an increase in the slope of the breakthrough curve) and a decrease in the time required to achieve breakthrough. For column I, since bed height is of the order of the adsorption zone length, the adsorption zone is at the bed bottom from the beginning of the run and the predominating effect of increase in zone speed at higher HLR is not of much relevance. For the 600 mm run, however, this effect is of importance and results in the observed variation in adsorption capacity at high HLR. The relative contribution of the various resistances at different HLR, are given in Table 6.

The same explanation accounts for the increase in minimum effluent concentration with HLR starting from less than 1 mg/l at HLR of 12 $m^3/h/m^2$ to more than 3 mg/l at 24 $m^3/h/m^2$ for a 600 mm bed. The slope of the 300 mm bed curve is steeper showing a greater sensitivity to HLR.

### 4.3. *Effect of bed height*

Set III experiments on effect of bed height showed an exponential decrease in minimum effluent concentration with bed height, keeping other parameters constant (Fig. 7). The minimum effluent concentration decreases rapidly from 12 mg/l for a bed height of 200 mm to around 4 mg/l for 300 mm bed height, beyond which the decrease is gradual, reaching below 1 mg/l for a bed height of about 700 mm. Beyond a bed height of 800 mm, the curve shows no appreciable change in minimum effluent concentration with further increase in bed height.

As the bed height increases, the length of the bed though which the effluent passes increases. There is no change in the adsorption zone length or in the speed of the zone. The increase in the total adsorptive capacity of the bed results in a decrease in the solute concentration in the effluent. The change in the slope of the curve with increasing bed height can be explained, again on the basis of mass transfer processes. For small bed heights, where the adsorption zone is of the order of the bed height, the adsorption zone reaches the bed bottom near the beginning of the run, resulting in a rapid rise in effluent concentrations right from the start. As the bed height increases much beyond the length of the adsorption zone, an appreciable period of time elapses before the zone reaches bed bottom. As such, low effluent concentrations are obtained in the beginning of the run. Further, as the ratio of bed height to zone length increases beyond 2, the effluent concentrations obtained in the initial time period will be nearly independent of the bed height.

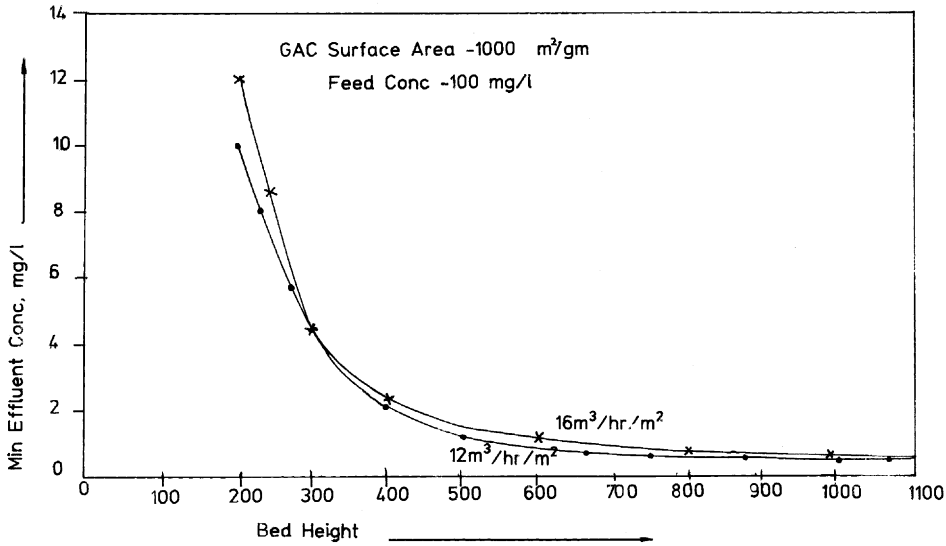


Fig. 7. Minimum effluent concentration vs. GAC bed height for TNT.

Limited results available for effect of bed height on adsorption capacity show that the relationship is not proportional. The adsorption capacity increases from 128 mg/g for a 300 mm bed to about 188 mg/g for a 600 mm bed at a HLR of 12 $m^3/h/m^2$ and feed concentration of 100 mg/l. From Table 7, it is seen that doubling the bed height leads to an increase of only 57% in total adsorption capacity. Comparison of columns I and II adsorption capacities shows a distinct improvement in the latter. This is because the TNT loading rate is lower for the second column as compared to first column. Further, the increase in adsorption capacity for column II as compared to column I is nearly 94% at low HLR and decreases rapidly at higher HLR. On the other hand, at high HLR, the combined capacity of columns I and II is higher, 341 and 264 mg/g, as compared to 248 mg/g at a HLR of 12 $m^3/h/m^2$. For practical purposes, the total adsorption capacity is important.

In addition, it is preferable that column II should be nearly virgin (effluent from second column should not exceed permissible discharge limits) when the first column gets exhausted. Both conditions of high total adsorption capacity and low saturation of column II are met for a HLR of 16 $m^3/h/m^2$ with the specified minimum bed heights. Therefore, this was selected as an optimal HLR for operation.

Table 7
Effect of GAC bed height on adsorption capacity

| Bed height (mm) | 300 (column I) | | | 600 (column I + II) | | | 300 (column II) | | |
|---|---|---|---|---|---|---|---|---|---|
| HLR ($m^3/h/m^2$) | 12 | 16 | 24 | 12 | 16 | 24 | 12 | 16 | 24 |
| Adsorption capacity (mg/gm) | 128 | 267 | 224 | 188 | 304 | 244 | | | |
| Increase in adsorption capacity (%) | 57 | 14 | 9 | 248 | 341 | 264 | 94 | 20 | 15 |
| Adsorption capacity (column II) consumed at breakthrough (%) | | | | | | | 3 | 3.5 | 20 |

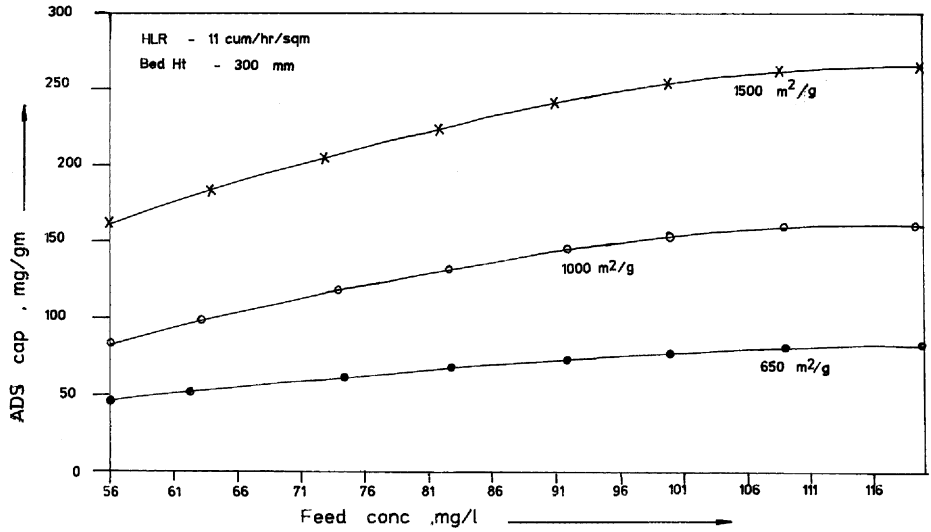


Fig. 8. Adsorption capacity vs. feed concentration for TNT.

### 4.4. Effect of feed concentration

Results from Set IV experiments with variable feed concentration are given in Fig. 8. Fig. 8 depicts the variation in adsorption capacity with feed concentration for various grades of GAC. The adsorption capacity shows an appreciable increase with feed concentration for higher grades of GAC, but the rise in case of grade 6 is marginal. Further, for feed concentrations higher than 100 mg/l, the rise in adsorption capacities, even for the higher grades, is negligible. As feed concentration increases, TNT loading rate increases, but so does the driving force for mass transfer, so that the NTUs decreases and therefore the adsorption zone length decreases. The net effect is an appreciable increase in adsorption capacity. But for feed concentrations >100 mg/l, while the loading rate uniformly increases with the feed concentration, the driving force does not increase at the same rate as is borne out from its isotherm adsorption behaviour [5]. The net result is a decrease in the adsorption capacity.

Comparison may be made between the cases of effect of low feed concentration to first column and comparatively low loading rate in second column. In the case of the former, since the feed concentration in a particular run remains constant, while the bed gets more and more saturated, the net driving force for mass transfer decreases with time. In case of the latter, on the other hand, the driving force remains nearly constant, because both the loading rate to column II and the saturation of GAC in the column increase with the run. Therefore, an increase in adsorption capacity is observed, in contrast to the case of low feed concentrations to column I.

The minimum effluent concentration increases with feed concentration for various grades of GAC. But, the effect is appreciable only at feed concentrations above 100 mg/l and for

Table 8
Comparison of model predictions with experimental data

| Nitro-organic | Feed concentration (mg/l) | Bed height (mm) | Breakthrough time (h) | | |
|---|---|---|---|---|---|
| | | | Hydraulic loading rate ($m^3/h/m^2$) | | |
| | | | 15 | 21 | 27 |
| Nitrobenzene | | | | | |
| Calculated | 200 | 300 | 19.5 | 13.1 | 9.2 |
| Experimental | 200 | 300 | 20 | 16.5 | 9 |
| Trinitrotoluene | | | | | |
| Calculated | 100 | 300 | 13 | 24.7 | 14.2 |
| | | 600 | 47 | 58.3 | 35 |
| Experimental | 100 | 300 | 15 | 25 | 14 |
| | | 600 | 47 | 57 | 30.5 |
| Dinitrotoluene | | | | | |
| Calculated | 33 | 300 | 21 | 27.8 | 21.3 |
| Experimental | 33 | 300 | 20 | 28 | 22 |

lower grades of GAC. For GAC of higher grade, the increase in surface area of the bed and correspondingly, the adsorption capacity, compensates for the increase in adsorption zone length, so that the breakthrough does not occur any sooner and therefore, the minimum $c_e$ is not much affected.

### 4.5. Comparison of experimental results with model predictions

Table 8 compares experimentally obtained breakthrough times with model predictions. It is seen that there is a very good agreement between the two, thereby validating the model.

### 4.6. Comparison of other nitro-organics with TNT

Figs. 9 and 10 show the adsorption behaviour of the other nitro-organics studied, NB and DNT. Fig. 9 shows the effect of increase in HLR on the adsorption capacity. NB shows the maximum adsorption capacity corresponding to a particular HLR followed by TNT and DNT.

These observations may be explained by considering the structure of the corresponding molecules. NB is a small, polar molecule with a nitro group. All these factors serve to improve the adsortion of NB on GAC. The three nitro groups in TNT tend to increase the adsorption on GAC but the effect of the large molecular size, which restricts its entry into smaller pores leads to a somewhat lower adsorption capacity for TNT compared to NB but higher than that of DNT with only two nitro groups.

Fig. 10 gives the variation in minimum effluent concentration ($c_{e,min}$) with bed height of GAC. It is observed that DNT has the highest $c_{e,min}$ for a specific bed height, followed by TNT and NB, respectively. This follows from the better adsorption characteristics of GAC for NB, followed by TNT and DNT, in that order.

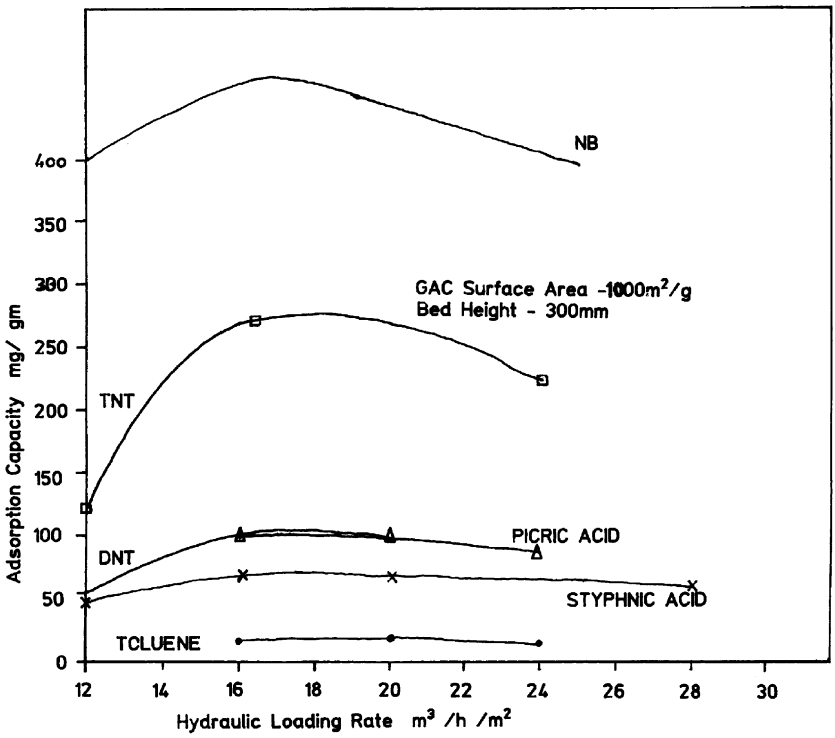


Fig. 9. Adsorption capacity vs. HLR for various nitro-organics.

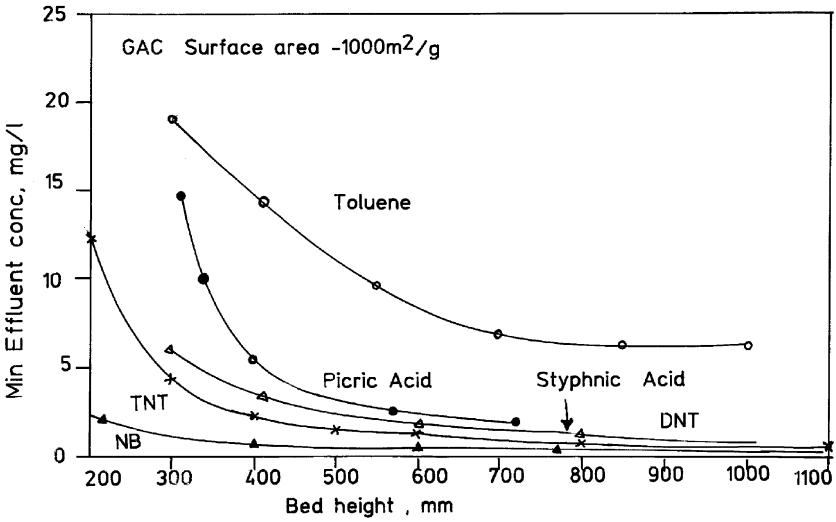


Fig. 10. Minimum effluent concentration vs. GAC bed height for various nitro-organics.

A study of the comparative effect of varying feed concentration on the adsorption behaviour of the nitro-organics shows similar behaviour. However, NB is observed to be most sensitive to the variation in feed concentration, showing a rapid rise in $c_{e,min}$ with feed concentration while DNT is least sensitive, showing only a marginal increase in $c_{e,min}$ under similar conditions.

### 4.7. Results from mixture studies

The composition of the synthetic mixture prepared for these studies was based on the analysis of the actual effluent from a TNT manufacturing plant. The results of the analysis carried out using HPLC are depicted in Fig. 11. The breakthrough curves for the mixture and for each of the components — NB, TNT and DNT, obtained on the basis of these experiments is given in Fig. 12. A comparison of the individual breakthrough curves shows that the breakthrough time is maximum for NB (28 h) and minimum for TNT (24 h). The breakthrough time for the mixture corresponds to that of TNT which is as expected, as TNT forms the major component of the mixture (79%). The adsorption capacities calculated on the basis of the breakthrough curves are 10 mg/l for NB, 40 mg/l for DNT and 167 mg/l for TNT. The adsorption capacity for the mixture is 216 mg/l, which corresponds to the sum of the individual adsorption capacities of the nitro-bodies in the mixture, establishing

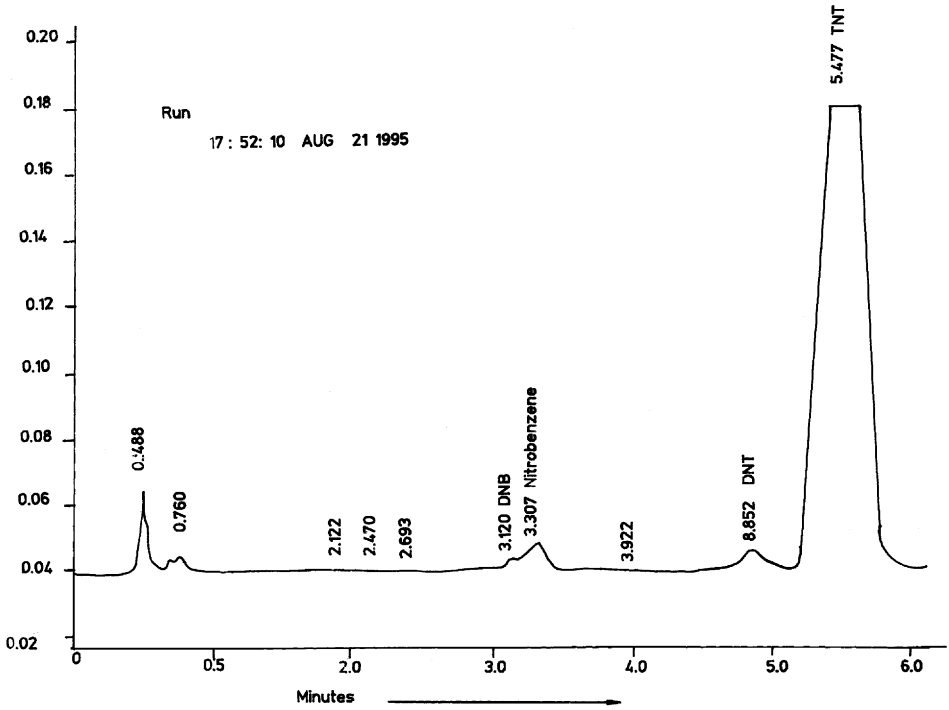


Fig. 11. HPLC analysis of effluent from TNT manufacturing plant.

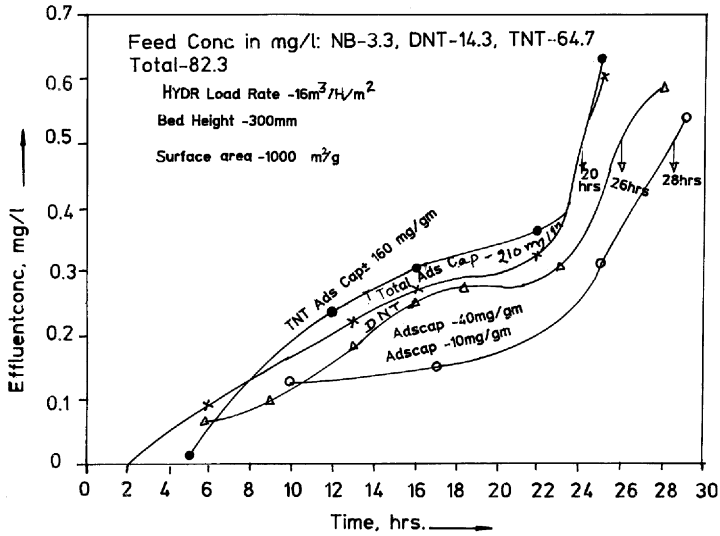


Fig. 12. Breakthrough curves for NB, DNT and TNT in mixture.

the additive nature of this property. Further, the ratio of adsorption capacities obtained for the individual components are in the ratio of their concentrations in the mixture. Fig. 13 compares the breakthrough curves obtained from experimental runs with TNT in single component and in mixture. Comparison of the two curves shows that the effluent TNT concentrations are initially comparatively lower for the mixture, showing better adsorption. After a run of 4–5 h, however, the trend starts to reverse. The adsorption characterisitcs for the single component solution are markedly better leading to better adsorption capacities

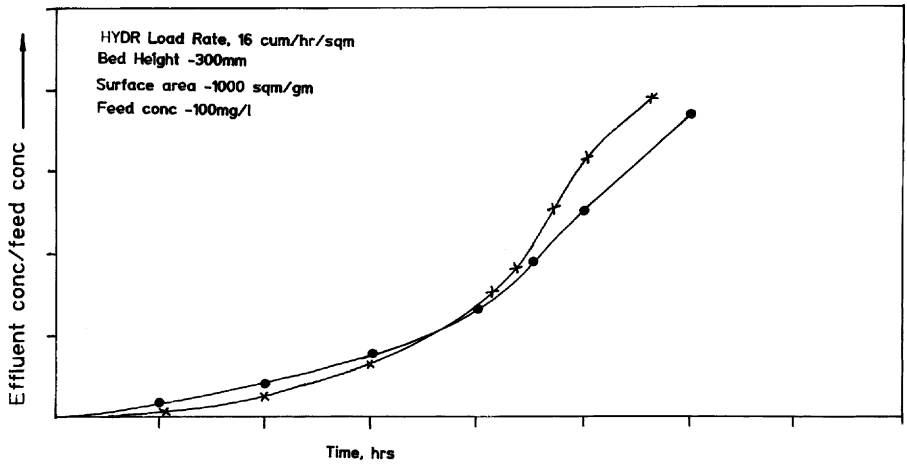


Fig. 13. Comparison of breakthrough curve for TNT in single component solution and in mixture.

on the whole. Similar results were observed in case of NB and DNT. The decrease in adsorption capacity in the mixture is observed for all three cases, being maximum for NB. This behaviour indicates that in the initial stages (when the GAC bed is virgin), the presence of other nitrobodies does not inhibit the adsorption of individual components of the mixture. But as more and more sites get occupied, competitive adsorption comes into play, resulting in the observed decrease in adsorption capacity for each component in the mixture.

### *4.8. Conclusion from bench scale studies*

Based on the results of column experiments, the GAC grade was optimised at 1000 $m^2/g$ and the feed concentration at 100 mg/l. The minimum bed height required to achieve permissible levels of nitrobody concentrations in a treated effluent was found to be around 800 mm, while the optimum HLR was found to lie between 16 and 20 $m^3/h/m^2$ in order to maximise the adsorption capacity of GAC. On the basis of these optimisation studies and an adsorption model developed to predict breakthrough behaviour [1], a pilot plant for the treatment of effluent waste waters from a TNT production plant was designed and constructed and is now in operation.

## Acknowledgements

The authors are indebted to the Director, Centre for Environment and Explosive Safety, DRDO, Metcalfe House, New Delhi, for his invaluable guidance and steady encouragement in the pursuit of this work.

## References

[1] C. Rajagopal, K. Misra, J.C. Kapoor, Development of a dynamic adsorption process for removal of nitro-bodies using GAC, in: Proceedings of the International Carbon Congress, Indian Carbon Society, Kanpur, India, December 1996.

[2] C. Rajagopal, J.C. Kapoor, Environmental effects of toxic nitro-organics and their removal from effluent waste-waters by dynamic column adsorption on GAC, in: Proceedings of the International Congress on Ergonomics, Health, Safety and Environment, DIPAS, DRDO, Delhi, November 1996.

[3] Effluent Standards for Environmental Pollutants, US Chemical Industry Digest Consultancy, Special Issue II, 1991.

[4] Granular activated carbon (GAC) system performance capabilities and optimisation, Report No. AMXTHTE C R 87111, USATHAMA, USA, February 1987.

[5] S.K. Kapoor, J.C. Kapoor, K. Shipra Mishra, P. Agarwal, A.K. Bhalla, R.C. Bansal, Studies on adsorption of nitro-compounds on activated carbon, in: Proceedings of the 2nd National Congress on Carbon, Indian Carbon Society, Bhopal, 1994.

[6] R.E. Treybal, Mass Transfer Operations, Student Edition, McGraw-Hill, New York, 1973, pp. 503–511.

[7] R.A. Perry, C.H. Chilton, Chemical Engineers Handbook, 5th Edition, McGraw-Hill, New York, 1973, pp. 16–23.